

# Some complexity measures in confined isotropic harmonic oscillator

Neetik Mukherjee and Amlan K. Roy\*

*Department of Chemical Sciences*

*Indian Institute of Science Education and Research (IISER) Kolkata,*

*Mohanpur-741246, Nadia, WB, India*

## Abstract

Various well-known statistical measures like *López-Ruiz, Mancini, Calbet* (LMC) and *Fisher-Shannon* complexity have been explored for confined isotropic harmonic oscillator (CHO) in composite position ( $r$ ) and momentum ( $p$ ) spaces. To get a deeper insight about CHO, a more generalized form of these quantities with Rényi entropy ( $R$ ) is invoked here. The importance of scaling parameter in the exponential part is also investigated.  $R$  is estimated considering order of entropic moments  $\alpha, \beta$  as  $(\frac{2}{3}, 3)$  in  $r$  and  $p$  spaces respectively. Explicit results of these measures with respect to variation of confinement radius  $r_c$  is provided systematically for first eight energy states, namely,  $1s$ ,  $1p$ ,  $1d$ ,  $2s$ ,  $1f$ ,  $2p$ ,  $1g$  and  $2d$ . Detailed analysis of these complexity measures provides many hitherto unreported interesting features.

**PACS:** 03.65-w, 03.65Ca, 03.65Ta, 03.65.Ge, 03.67-a.

**Keywords:** *LMC* complexity, *Fisher-Shannon* complexity, Rényi entropy, Shannon entropy, Confined isotropic harmonic oscillator.

---

\*Corresponding author. Email: akroy@iiserkol.ac.in, akroy6k@gmail.com.

## I. INTRODUCTION

Quantum particles undergo dramatic changes in their chemical and physical properties under extreme pressure. Such situations may be achieved by shifting their spatial boundary from infinity to finite region [1]. The effect of boundary condition and boundary limit on various observable properties such as energy spectrum, transition frequency, transition probability, polarizability, chemical reactivity, ionization potential etc., were studied in considerable detail in last ten years [2, 3]. These systems have their comprehensive and potential application in nano-science and technology, condensed matter physics, semiconductor physics, quantum dot, quantum wells and quantum wires, etc [2, 3].

From the beginning of this century there has been a thriving interest in exploring statistical quantities namely, Fisher information ( $I$ ), Onicescu energy ( $E$ ), Shannon entropy ( $S$ ) and Rényi entropy ( $R$ ) as signifier of certain chemical, physical properties of a quantum system. In the same direction, *complexity*, another topical concept, is directly concerned to aforesaid measures and illustrates their combined effect. A global definition of complexity has not yet been possible. But it may be treated as a demonstrator of pattern, structure or correlation related with the distribution function in a given system. It depends on the scale of inspection, and comprises an important area of investigation with contemporary interest in chaotic systems, spatial patterns, language, multi-electronic systems, molecular or DNA analysis, social science, astrophysics and cosmology [4–7] etc.

A quantum harmonic oscillator is a complex system; circumscribing its oscillation within an impenetrable region makes it even more impressive according to a complex world [8, 9]. Complexity, in a system, is introduced by disrupting certain rules of symmetry. A system possesses finite complexity when it is either in a state having less than some maximal order or not at a state of equilibrium. In a nutshell, it vanishes at two limiting cases, *viz.*, when a system is (i) completely ordered (maximum distance from equilibrium) or (ii) at equilibrium (maximum disorder) [9]. Overall it provides a characteristic idea of distribution in a system and is deliberated as a general descriptor of structure and correlation. In literature several definitions are available; some of them are Shiner, Davidson, Landsberg (*SDL*) [10–12], López-Ruiz, Mancini, Calbet (LMC) *shape* ( $C_{LMC}$ ) [13–16], *Fisher-Shannon* ( $C_{IS}$ ) [17–19], *Cramér-Rao* [19–21] or *Generalized Rényi-like* complexity [22–25], generalized relative complexity measures [26] etc.

Without any loss of generality, the statistical measure of complexity, may be defined as a product of ordered and disordered parameters in the following form,

$$C_{LMC} = H.D, \quad (1)$$

where  $H$  represents the information content and  $D$  narrates an idea of concentration of spatial distribution. For a normalized continuous distribution  $p(\mathbf{r})$  these two quantities were expressed [13] in the form  $H = -k \int p(\mathbf{r}) \log p(\mathbf{r}) d\mathbf{r}$  ( $k$  is a positive constant) and  $D = \int p^2(\mathbf{r}) d\mathbf{r}$ . But, this definition of  $C_{LMC}$  was criticized [27] due to its inability to satisfy necessary conditions such as reaching minimal values for both extremely ordered and disordered limits, invariance under scaling, translation and replication. Therefore, this model was modified [28], giving rise to the expression,

$$C_{LMC} = D.e^S. \quad (2)$$

Here,  $S$  quantifies the information of a given system and has the mathematical form  $-\int p(\mathbf{r}) \log p(\mathbf{r}) d\mathbf{r}$ . Principally  $C_{LMC}$  quantifies the interaction between intrinsic information hidden in a system, and measure of a probabilistic distribution amongst its observed parts. It has potential application in several fields like detection of periodic, quasi-periodic, linear stochastic, chaotic dynamics [13, 29, 30] and in quantum phase transition [31, 32].

In information theory  $E$  measures information content of a system. It sets off to minimum at equilibrium. Hence  $E$  signifies a descriptor of order. Whereas information entropies like  $S, R$ , become maximum at equilibrium, thereby implying disorder. Complexity quantifies the extent of countervail between order and disorder. In many instances,  $E$  is replaced by  $I$ . So far in the literature  $S$  has been primarily used as disorder parameter.  $C_{IS}$  is another measure, attained by changing the pre-exponential global factor in  $C_{LMC}$  by a local factor like  $I$ . It unites global and local characters while conserving the characteristics of complexity. Effectiveness of  $C_{IS}$  can be reviewed by looking at numerous literature available for both *free* and *confined* atomic systems, including atomic shell structure, ionization process [18, 19, 21, 33, 34] etc. Recently a more generalized version was also designed that uses  $R$  in place of  $S$ , in  $C_{LMC}$  and  $C_{IS}$  [9]. Later, a scaling factor ( $b$ ) was invoked in exponential part.

About a decade ago, both  $C_{LMC}$  and  $C_{IS}$  were explored in the context of Bohr-like states of *free* isotropic harmonic oscillator (IHO) in  $r, p$  spaces [35]. However, in *confined* environment  $LMC$  complexity has been investigated only for ground state of some model

systems, like, CHO, confined h-atom, particle in spherical box and confined Helium atom [36, 37]. Very recently, the present authors have pursued similar calculations for confined hydrogen atom [38] and found that, parameter  $b$  plays a key role in interpreting the property of a system. In this endeavor, our objective is to explore four different types of complexity emerging out of two order ( $I, E$ ) and two disorder ( $S, R$ ) parameters, in conjugate spaces, as functions of confinement radius ( $r_c$ ). We take into account two  $b$  values available in literature [9], and these are ( $\frac{2}{3}$  for  $C_{IS}$ , 1 for  $C_{LMC}$ ). All calculations were carried out using *exact* wave functions of CHO in  $r$  space. The  $p$ -space wave function is computed by applying numerical Fourier transform of  $r$ -space counterpart. In the end, representative calculation are done for eight low-lying states *viz.*,  $1s$ ,  $1p$ ,  $1d$ ,  $2s$ ,  $1f$ ,  $2p$ ,  $1g$  and  $2d$ . Presentation of the article is as follows. Section II gives a brief outline of the theoretical method used; Sec. III presents a thorough discussion on our results, while we conclude with a few remarks in Sec. IV.

## II. METHODOLOGY

The time-independent, non-relativistic wave function for a CHO system, in  $r$  space can be written as,

$$\Psi_{n,l,m}(\mathbf{r}) = \psi_{n,l}(r) Y_{l,m}(\Omega), \quad (3)$$

with  $r$  and  $\Omega$  representing radial distance and solid angle successively. Here  $\psi_{n,l}(r)$  denote the radial part and  $Y_{l,m}(\Omega)$  identifies spherical harmonics. The latter has following common form in both  $r$  and  $p$  spaces ( $P_l^m(\cos \theta)$  denotes usual associated Legendre polynomial),

$$Y_{l,m}(\Omega) = \Theta_{l,m}(\theta) \Phi_m(\phi) = (-1)^m \sqrt{\frac{2l+1}{4\pi} \frac{(l-m)!}{(l+m)!}} P_l^m(\cos \theta) e^{-im\phi}. \quad (4)$$

The relevant radial Schrödinger equation under the influence of confinement is,

$$\left[ -\frac{1}{2} \frac{d^2}{dr^2} + \frac{l(l+1)}{2r^2} + v(r) + v_c(r) \right] \psi_{n,l}(r) = \mathcal{E}_{n,l} \psi_{n,l}(r), \quad (5)$$

where  $v(r) = \frac{1}{2}\omega^2 r^2$  and  $\omega$  is the oscillator frequency. Our required confinement effect is induced by invoking the following form of potential:  $v_c(r) = +\infty$  for  $r > r_c$ , and 0 for  $r \leq r_c$ , where  $r_c$  denotes radius of confinement.

*Exact* generalized radial wave function for a CHO is mathematically expressed as [39],

$$\psi_{n_r,l}(r) = N_{n_r,l} r^l {}_1F_1 \left[ \frac{1}{2} \left( l + \frac{3}{2} - \frac{\mathcal{E}_{n_r,l}}{\omega} \right), \left( l + \frac{3}{2} \right), \omega r^2 \right] e^{-\frac{\omega}{2} r^2}. \quad (6)$$

Here,  $N_{n,l}$  represents normalization constant and  $\mathcal{E}_{n,l}$  corresponds to the energy of a given state distinguished by quantum numbers  $n, l$ , whereas  ${}_1F_1[a, b, r]$  represents confluent hypergeometric function. Allowed energies are obtained by applying the boundary condition  $\psi_{n,\ell}(0) = \psi_{n,\ell}(r_c) = 0$  (except for  $l = 0$  states, only  $\psi_{n,\ell}(r_c) = 0$ ). In this work, generalized pseudospectral (GPS) method was employed to calculate  $\mathcal{E}_{n,l}$  of these states. This method has provided very accurate results for various model and real systems including atoms, molecules, some of which could be found in the references [40–42]. This is very well documented and therefore omitted here.

The  $p$ -space wave function is obtained from Fourier transform of  $r$ -space counterpart,

$$\begin{aligned}\psi_{n,l}(p) &= \frac{1}{(2\pi)^{\frac{3}{2}}} \int_0^{r_c} \int_0^\pi \int_0^{2\pi} \psi_{n,l}(r) \Theta(\theta) \Phi(\phi) e^{ipr \cos \theta} r^2 \sin \theta \, dr d\theta d\phi \\ &= \frac{1}{2\pi} \sqrt{\frac{2l+1}{2}} \int_0^{r_c} \int_0^\pi \psi_{n,l}(r) P_l^0(\cos \theta) e^{ipr \cos \theta} r^2 \sin \theta \, dr d\theta.\end{aligned}\quad (7)$$

Here  $\psi(p)$  is not normalized and needs to be normalized. Integrating over  $\theta$  and  $\phi$  yields,

$$\psi_{n,l}(p) = (-i)^l \int_0^{r_c} \frac{\psi_{n,l}(r)}{p} f(r, p) dr. \quad (8)$$

$f(r, p)$  depends only on  $l$  quantum number. It can be expressed in terms of *Cos* and *Sin* series. More details about  $f(r, p)$  could be found in [43].

The normalized position and momentum electron densities are expressed as,

$$\rho(\mathbf{r}) = |\psi_{n,l,m}(\mathbf{r})|^2, \quad \Pi(\mathbf{p}) = |\psi_{n,l,m}(\mathbf{p})|^2. \quad (9)$$

Without any loss of generality, let us express complexity in a generalized mathematical form as  $C = Ae^{bB}$ . The order ( $A$ ) and disorder parameters ( $B$ ) may comprise of ( $E, I$ ) and ( $R, S$ ) respectively. With this in mind, we are interested in the following four quantities,

$$C_{ER} = Ee^{bR}, \quad C_{IR} = Ie^{bR}, \quad C_{ES} = Ee^{bS}, \quad C_{IS} = Ie^{bS}. \quad (10)$$

Shannon entropy of a continuous density distribution is written as ('t' stands for *total*),

$$S_{\mathbf{r}} = - \int_{\mathcal{R}^3} \rho(\mathbf{r}) \ln[\rho(\mathbf{r})] \, d\mathbf{r}; \quad S_{\mathbf{p}} = - \int_{\mathcal{R}^3} \Pi(\mathbf{p}) \ln[\Pi(\mathbf{p})] \, d\mathbf{p}; \quad S_t = S_{\mathbf{r}} + S_{\mathbf{p}}. \quad (11)$$

Similarly, Rényi entropy of order  $\alpha (\neq 1)$  is obtained by taking logarithm of  $\alpha$  and  $\beta$ -order entropic moments in respective spaces [9],

$$R_{\mathbf{r}}^\alpha = \frac{1}{1-\alpha} \ln \left( \int_{\mathcal{R}^3} \rho^\alpha(\mathbf{r}) d\mathbf{r} \right); \quad R_{\mathbf{p}}^\beta = \frac{1}{1-\beta} \ln \left[ \int_{\mathcal{R}^3} \Pi^\beta(\mathbf{p}) d\mathbf{p} \right]; \quad R_t = R_{\mathbf{r}}^\alpha + R_{\mathbf{p}}^\beta. \quad (12)$$

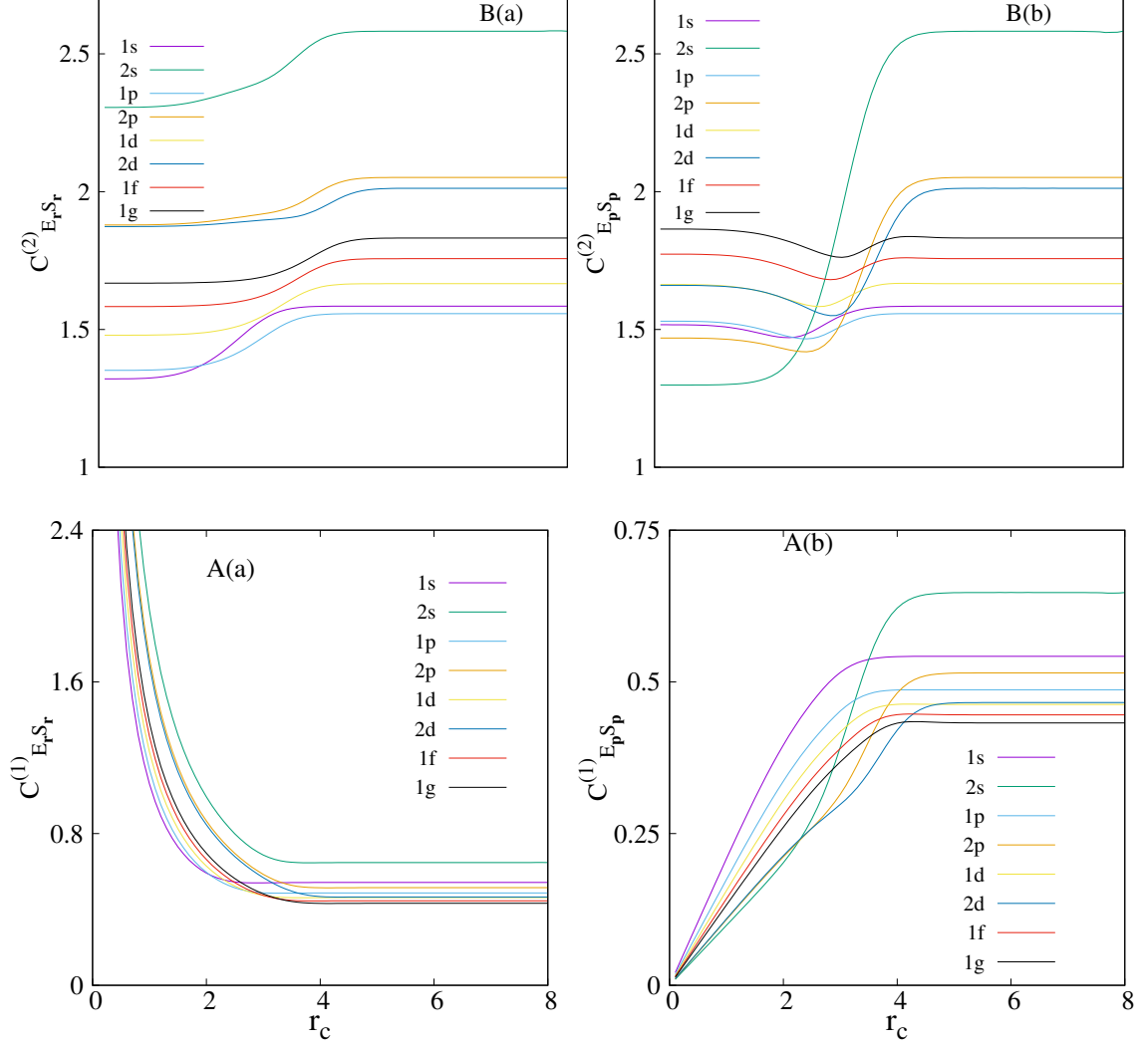


FIG. 1: Variation of  $C_{E_r S_r}^{(1)}$ ,  $C_{E_p S_p}^{(1)}$  (bottom row A) and  $C_{E_r S_r}^{(2)}$ ,  $C_{E_p S_p}^{(2)}$  (top row B) in CHO with  $r_c$  for  $1s, 1p, 1d, 2s, 1f, 2p, 1g, 2d$  states. See text for details.

where,

$$\frac{1}{\alpha} + \frac{1}{\beta} = 2$$

$I_r, I_p$  for a particle in a central potential may be expressed as [44],

$$I_r = 4\langle p^2 \rangle - 2(2l + 1)|m|\langle r^{-2} \rangle; \quad I_p = 4\langle r^2 \rangle - 2(2l + 1)|m|\langle p^{-2} \rangle; \quad I_t = I_r I_p. \quad (13)$$

Finally,  $E$  is given by the following expressions in conjugate space [9],

$$E_r = \int_{\mathcal{R}^3} \rho^2(\mathbf{r}) d\mathbf{r}; \quad E_p = \int_{\mathcal{R}^3} \Pi^2(\mathbf{p}) d\mathbf{p}; \quad E_t = E_r E_p. \quad (14)$$

TABLE I:  $C_{E_r S_r}^{(1)}$ ,  $C_{E_p S_p}^{(1)}$  and  $C_{E_t S_t}^{(2)}$  for  $1s$ ,  $2s$ ,  $1p$ ,  $1d$  states in CHO at various  $r_c$ .

$r_c$	$C_{E_r S_r}^{(1)}$	$C_{E_p S_p}^{(1)}$	$C_{E_t S_t}^{(1)}$	$C_{E_r S_r}^{(1)}$	$C_{E_p S_p}^{(1)}$	$C_{E_t S_t}^{(1)}$
	$1s$			$2s$		
0.1	10.544267	0.02093	0.22073	19.769038	0.00985	0.19491
0.2	5.272192	0.04186	0.22074	9.8845272	0.01972	0.19499
0.5	2.1098387	0.10464	0.22079	3.9539382	0.04933	0.19504
0.8	1.3220786	0.16721	0.22106	2.4716592	0.07894	0.19513
1.0	1.0623420	0.20854	0.22154	1.9779193	0.09871	0.19525
2.5	0.5453416	0.46594	0.25409	0.7991488	0.27391	0.21889
5.0	0.5422182	0.54221	0.29399	0.6472847	0.64698	0.41878
7.0	0.5422182865	0.5422182865	0.2940006701	0.6472880855	0.6472825716	0.4189782966
	$1p$			$1d$		
0.1	11.363226	0.01746	0.19849	12.302938	0.01561	0.19216
0.2	5.6816369	0.03493	0.19850	6.1514809	0.03123	0.19217
0.5	2.2730425	0.08733	0.19850	2.4607796	0.07809	0.19216
0.8	1.4220367	0.13961	0.19853	1.5386569	0.12487	0.19213
1.0	1.1395261	0.17426	0.19857	1.2318435	0.15593	0.19208
2.5	0.5143143	0.40130	0.20639	0.5232749	0.36665	0.19186
5.0	0.4869827	0.48699	0.23715	0.4628145	0.46285	0.21421
7.0	0.4869829166	0.4869829186	0.237152362	0.4628158714	0.4628158704	0.2141985303

### III. RESULT AND DISCUSSION

At the onset it is convenient to point out a few points about this report. The *net* information measures in conjugate  $r$  and  $p$  space may be separated into radial and angular segments. In a given space, the results provided correspond to *net* measures including the *angular* contributions. One can transform the IHO to a CHO by pressing the radial boundary of former from infinity to a finite region. This change in radial environment does not affect the *angular* boundary conditions. Therefore, angular part of the information measures in unconfined and confined systems remain unaltered in both spaces. Further as we are solely focused in *radial* confinement, this will also not influence the characteristics of a given measure as one changes  $r_c$ . Throughout this report, magnetic quantum number  $m$  remains fixed to 0. All the discussed measures of Eq. (10) have been explored with change of  $r_c$ , choosing two different and widely used values of  $b$  ( $1, \frac{2}{3}$ ). Note that, for  $b = 1$ ,  $C_{ES}^{(2)}$  modifies to  $C_{LMC}$ ; similarly  $C_{IS}^{(1)}$  coincides with  $C_{IS}$  at  $b = \frac{2}{3}$ . In order to simplify the discussion, a few words may be devoted to the notation followed. A uniform symbol  $C_{order_s, disorder_s}^b$  is used; where the two subscripts refer to two order ( $E, I$ ) and disorder ( $S, R$ )

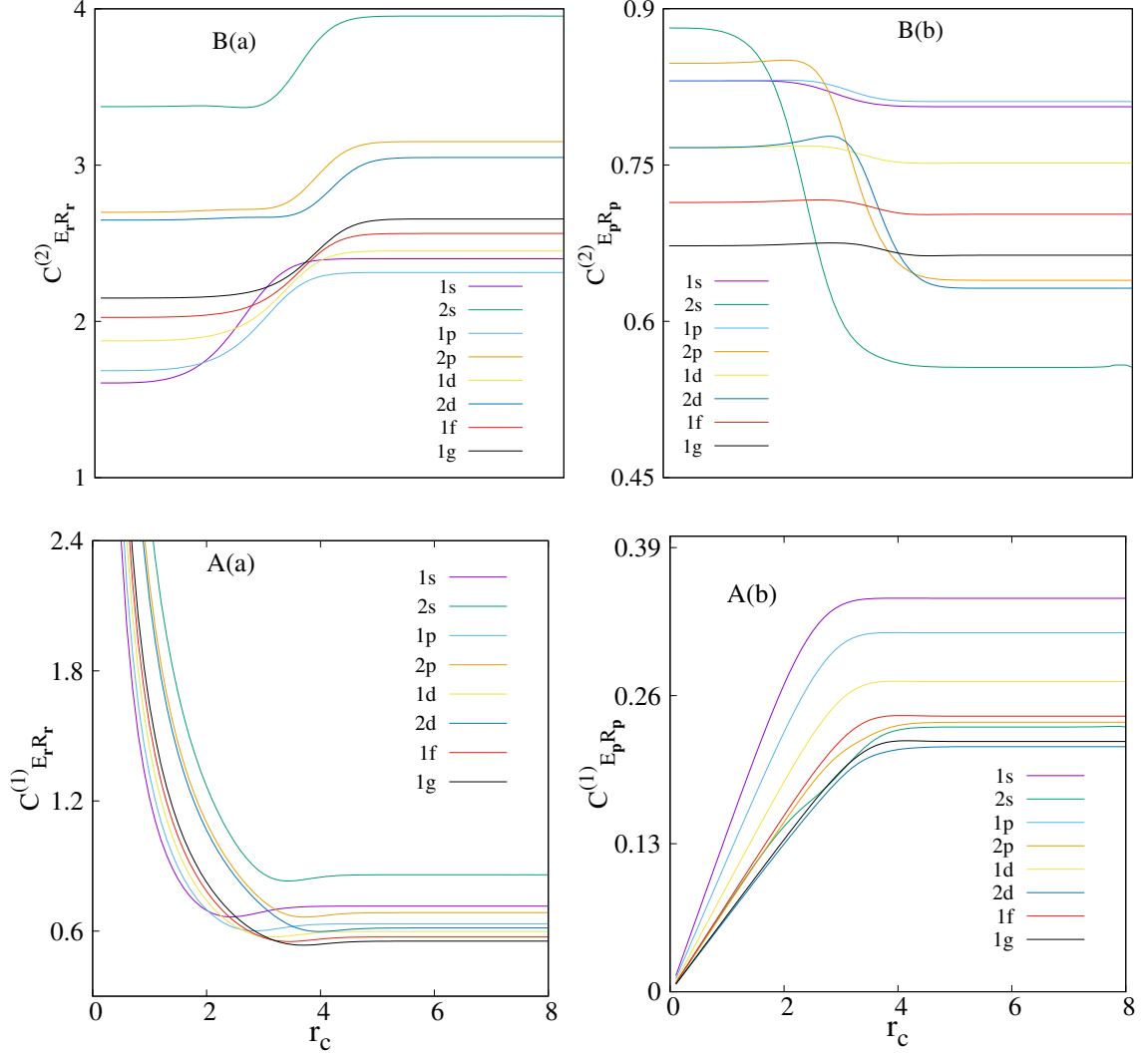


FIG. 2: Changes in  $C_{E_r R_r}^{(1)}$ ,  $C_{E_p R_p}^{(1)}$  (bottom row A) and  $C_{E_r R_r}^{(2)}$ ,  $C_{E_p R_p}^{(2)}$  (top row B) in CHO with  $r_c$  for  $1s, 1p, 1d, 2s, 1f, 2p, 1g, 2d$  states. For more details, see text.

parameters. Another subscript  $s$  is used to specify the space; *viz.*,  $r, p$  or  $t$  (total). Two scaling parameters  $b = \frac{2}{3}, 1$  are identified with superscripts (1), (2). These measures are offered systematically for  $1s, 1p, 1d, 2s, 1f, 2p, 1g$  and  $2d$  states in conjugate spaces, with  $r_c$  varying in the range of 0.1-8.0 a.u. Also it is important to point out that, here levels are denoted by  $n_r + 1$  and  $l$  values [45]. Therefore, as an example,  $n_r = 0, l = 1$  signify  $1p$  state, and  $n_r$  relates to  $n$  as  $n = 2n_r + l$ .

At first, in the bottom row (panels A(a)-A(b)) of Fig. 1,  $C_{E_r S_r}^{(1)}$ ,  $C_{E_p S_p}^{(1)}$  are plotted against  $r_c$  for all the eight states. Similarly, plots for  $C_{E_r S_r}^{(2)}$ ,  $C_{E_p S_p}^{(2)}$  are shown in panels B(a) and B(b) respectively. The lower panels clearly suggest that,  $C_{E_r S_r}^{(1)}$  decreases and  $C_{E_p S_p}^{(1)}$  increases



TABLE II:  $C_{E_r R_r}^{(1)}$ ,  $C_{E_p R_p}^{(1)}$  and  $C_{E_t R_t}^{(1)}$  for  $1s$ ,  $2s$ ,  $1p$ ,  $1d$  states in CHO at various  $r_c$ .

$r_c$	$C_{E_r R_r}^{(1)}$	$C_{E_p R_p}^{(1)}$	$C_{E_t R_t}^{(1)}$	$C_{E_r R_r}^{(1)}$	$C_{E_p R_p}^{(1)}$	$C_{E_t R_t}^{(1)}$
	$1s$			$2s$		
0.1	12.011965	0.01401	0.16830	25.481700	0.00761	0.19405
0.2	6.0060677	0.02802	0.16830	12.740847	0.01523	0.19415
0.5	2.4038079	0.07004	0.16838	5.0962894	0.03810	0.19417
0.8	1.5073076	0.11199	0.16881	3.1849974	0.06091	0.19401
1.0	1.2125775	0.13981	0.16953	2.5477258	0.07602	0.19369
2.5	0.6661575	0.31636	0.21074	1.0079698	0.16895	0.17030
5.0	0.7153170	0.34549	0.24713	0.8597424	0.23246	0.19985
7.0	0.7153219525	0.3454938391	0.2471393275	0.8599102013	0.2324933318	0.1999233878
	$1p$			$1d$		
0.1	13.160407	0.01162	0.15295	14.410589	0.00931	0.13429
0.2	6.5802381	0.02324	0.15296	7.2053113	0.01863	0.13430
0.5	2.6326593	0.05811	0.15298	2.8823989	0.04659	0.13431
0.8	1.6474274	0.09294	0.15312	1.8024800	0.07454	0.13435
1.0	1.3207023	0.11610	0.15334	1.4433285	0.09314	0.13443
2.5	0.6151214	0.27465	0.16894	0.6225095	0.22540	0.14031
5.0	0.6339254	0.31520	0.19981	0.5985573	0.27230	0.16299
7.0	0.6339446874	0.3152046743	0.1998223287	0.5986224459	0.2723045747	0.1630076305

with rise of  $r_c$  before reaching a threshold corresponding to the IHO. The decrease of  $C_{E_r R_r}^{(1)}$  with  $r_c$  points to its inclination towards equilibrium. Next, panel A(a) reveals that at a fixed  $l$ ,  $C_{E_r S_r}^{(1)}$  progresses with  $n$ . Conversely, at a particular  $n$ , it reduces with growth of  $l$ . But panel A(b) does not imprint such patterns for  $C_{E_p S_p}^{(1)}$ . Panel A(c) in Figure S1 of Supplementary Material (SM) presents that  $C_{E_t S_t}^{(1)}$  enhances with advancement of  $r_c$ . Now, panels B(a), B(b) delineate the variation of  $C_{E_r S_r}^{(2)}$ ,  $C_{E_p S_p}^{(2)}$  with change of  $r_c$ . One sees that,  $C_{E_r S_r}^{(2)}$  advances with growth of  $r_c$  indicating that this is more prone towards order. On the other hand, at first  $C_{E_p S_p}^{(2)}$  decreases with  $r_c$ , attains a minimum and finally coalesces to IHO. The ordering of  $C_{E_r S_r}^{(2)}$  regarding  $n$ ,  $l$  quantum numbers is akin to  $C_{E_r S_r}^{(1)}$ . It is noticed that, after a certain  $r_c$  ( $\gtrsim 3$ ), both  $C_{E_r S_r}^{(2)}$ ,  $C_{E_p S_p}^{(2)}$  show analogous nature (increase to reach their respective limiting value). Panel B(c) in Fig. S1 in SM portrays the increase of  $C_{E_t S_t}^{(2)}$  with  $r_c$ . By comparing these two sets of complexity measure, namely  $C_{ES}^{(1)}$  (in A(a)-A(c)) and  $C_{ES}^{(2)}$  (in B(a)-B(c)), it is evident that,  $C_{E_r S_r}^{(1)}$  and  $C_{E_p S_p}^{(1)}$  complement each other better (as former decreases and later increases with  $r_c$ ) than the other set. Hence, we have presented  $C_{E_r S_r}^{(1)}$ ,  $C_{E_p S_p}^{(1)}$  and  $C_{E_t S_t}^{(1)}$  at some selected  $r_c$  values in Table I, for  $1s$ ,  $2s$ ,  $1p$ ,  $1d$ . While for  $2p$ ,  $2d$ ,  $1f$ ,  $1g$  states these are produced in Table S1 of SM. These data consolidate the

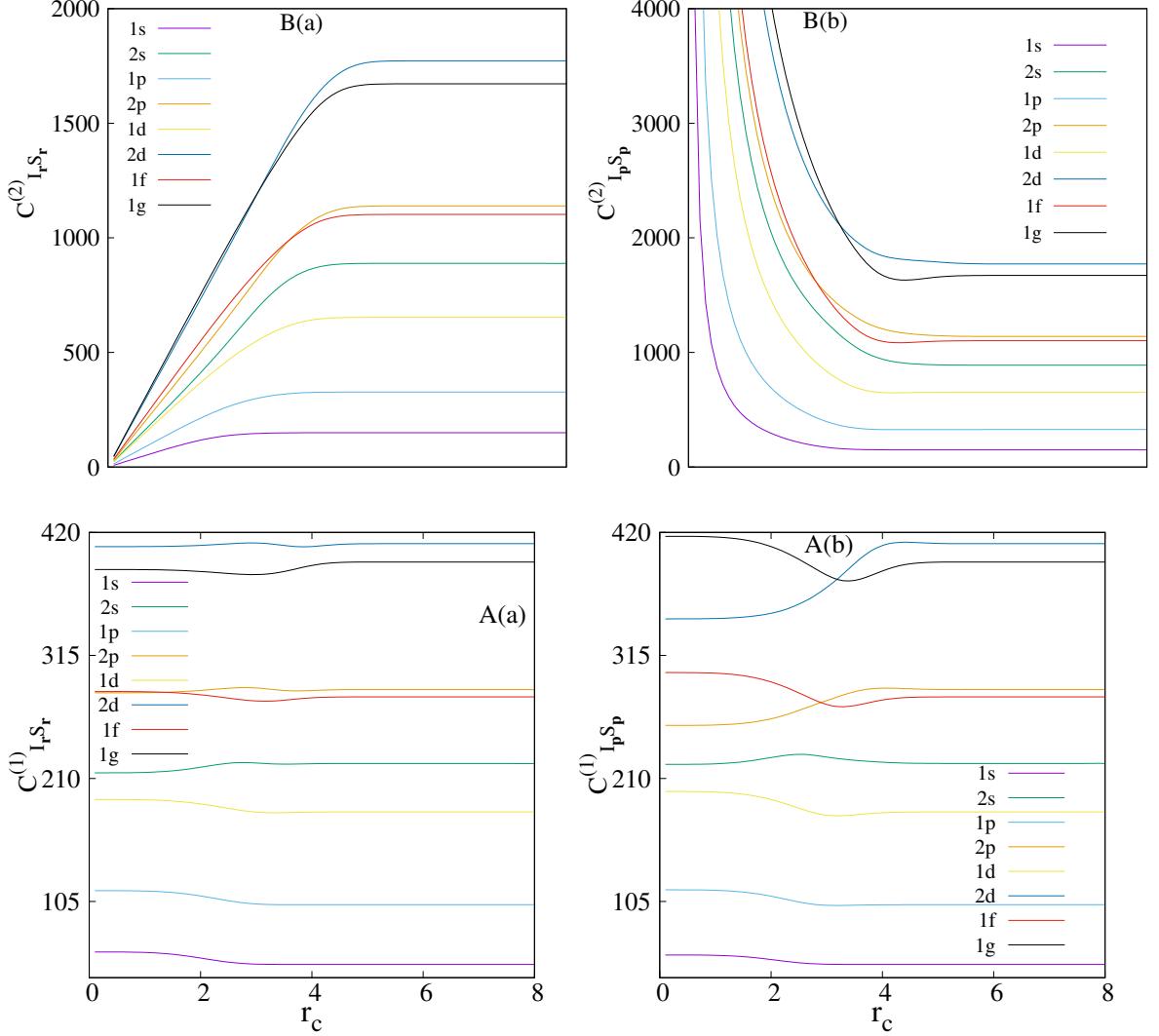


FIG. 3: Variation of  $C_{I_r S_r}^{(1)}$ ,  $C_{I_p S_p}^{(1)}$  (bottom row A)  $C_{I_r S_r}^{(2)}$ ,  $C_{I_p S_p}^{(2)}$  (top row B) in CHO with  $r_c$  for  $1s, 1p, 1d, 2s, 1f, 2p, 1g, 2d$  states. Consult text for more details.

inference drawn from Figs. 1 and S1. We also see that when CHO approaches to IHO,  $C_{E_r S_r}^{(1)}$  becomes equal to  $C_{E_p S_p}^{(1)}$ . None of these results could be directly compared with literature data, as no such works have been published before, to the best of our knowledge.

Similarly, bottom row of Fig. 2 interprets the behavior of  $C_{E_r R_r}^{(1)}$ ,  $C_{E_p R_p}^{(1)}$  with  $r_c$  for the same states of Fig. 1. Panel A(a) reveals that,  $C_{E_r R_r}^{(1)}$  diminishes with growth of  $r_c$ , then attains a minimum and finally converges to respective IHO result. This minimum gets flatter with progress of both  $n$ ,  $l$ . Here also  $C_{E_r S_r}^{(1)}$  shows analogous trend to what is noticed for  $C_{E_r S_r}^{(1)}$ , *viz.*, (i) at a fixed  $n$ , both measures in  $r$ -space decline with growth of  $l$  (ii) at a particular  $l$ , they accelerate with  $n$  (iii) like  $C_{E_r S_r}^{(1)}$ ,  $C_{E_r R_r}^{(1)}$  is more inclined towards

TABLE III:  $C_{I_r S_r}^{(2)}$ ,  $C_{I_p S_p}^{(2)}$  and  $C_{I_t S_t}^{(2)}$  for  $1s$ ,  $2s$ ,  $1p$ ,  $1d$  states in CHO at various  $r_c$ .

$r_c$	$C_{I_r S_r}^{(2)}$	$C_{I_p S_p}^{(2)}$	$C_{I_t S_t}^{(2)}$	$C_{I_r S_r}^{(2)}$	$C_{I_p S_p}^{(2)}$	$C_{I_t S_t}^{(2)}$
	$1s$			$2s$		
0.1	7.758205	4303.15991	33384.80018	25.056165	29216.5721	732055.2573
0.2	15.516171	2151.56736	33384.08737	50.112519	14608.3337	732060.4179
0.5	38.766040	860.42282	33355.18588	125.300544	5844.1079	732269.9114
0.8	61.804468	537.04703	33191.90621	200.655774	3655.3318	733463.4393
1.0	76.791106	428.68905	32919.50741	251.188685	2928.0196	735485.4165
2.5	145.231258	167.01717	24256.11393	663.377452	1216.9057	807267.8370
5.0	149.733084	149.73309	22419.99774	888.731009	888.9964	790078.7475
7.0	149.733087619267	149.73308721	22419.99746802	888.738383	888.7381	789855.7135
	$1p$			$1d$		
0.1	13.589616	10065.70616	136789.08528	23.086162	21178.15365	488922.29249
0.2	27.179055	5032.83116	136787.59609	46.172182	10589.04165	488919.15916
0.5	67.929622	2012.77692	136727.17589	115.415992	4235.04577	488792.00959
0.8	108.523492	1256.72638	136384.33569	184.533851	2644.87901	488069.71221
1.0	135.307764	1003.69056	135807.12614	230.387985	2113.17739	486850.68272
2.5	293.849512	382.32570	112346.22278	535.936973	802.82774	430265.07166
5.0	327.026856	327.02367	106945.52430	653.074539	653.04527	426487.24482
7.0	327.027007440	327.0270080	106946.6637782	653.077279415428	653.077279	426509.932617

disorder. From panel A(b) it is also vivid that, like  $C_{E_p R_p}^{(1)}$ ,  $C_{E_p R_p}^{(1)}$  progress with growth of  $r_c$ . Additionally, at a definite  $l$ ,  $C_{E_p R_p}^{(1)}$  falls off with  $n$ . At a given  $n$ , it also reduces as  $l$  advances. The relevant total measures are displayed in panel A(c) of Fig. S2 of SM, where prominent minima are seen for  $s$  states. As usual,  $C_{E_t R_t}^{(1)}$  finally merge to IHO case. Panels B(a), B(b) in top row of Fig. 2 exhibit variations of  $C_{E_r R_r}^{(2)}$ ,  $C_{E_p R_p}^{(2)}$  with  $r_c$ . At smaller  $r_c$  region ( $\lesssim 3$ ), they both change very slowly. At around  $r_c = 3$ ,  $C_{E_r R_r}^{(2)}$  jumps and  $C_{E_p R_p}^{(2)}$  drops to reach the IHO limit. For both  $C_{E_r R_r}^{(2)}$  and  $C_{E_p R_p}^{(2)}$  absolute values of the slope of the curve enhance as  $n$  grows (fixed  $l$ ) and decrease with growth of  $l$  (fixed  $n$ ). The dependence of  $C_{E_r R_r}^{(2)}$  on  $n$ ,  $l$  is similar to  $C_{E_r R_r}^{(1)}$ . Panel B(c) of Fig. S2 in SM imprints the alteration of  $C_{E_t R_t}^{(2)}$  with  $r_c$  varying from 0-8. Once again one may conclude that, out of  $C_{ER}^{(1)}$  and  $C_{ER}^{(2)}$ , the former offers a more clearer knowledge about CHO, which justifies the quantities produced in Table II, namely,  $C_{E_r R_r}^{(1)}$ ,  $C_{E_p R_p}^{(1)}$  and  $C_{E_t R_t}^{(1)}$ . These are given for  $1s$ ,  $1p$ ,  $2s$ ,  $1d$  states at eight suitably chosen  $r_c$ , whereas Table S2 reports the same for  $2p$ ,  $1f$ ,  $2d$ ,  $1g$  states. These results support the conclusions drawn from Figs. 2 and S2. Moreover it is also apparent that, there appears a minimum in  $C_{E_r R_r}^{(1)}$  for all states. Similar to previous table, in this case also no literature values could be quoted. Additionally,  $C_{E_p R_p}^{(1)}$  shows more lucid trend than

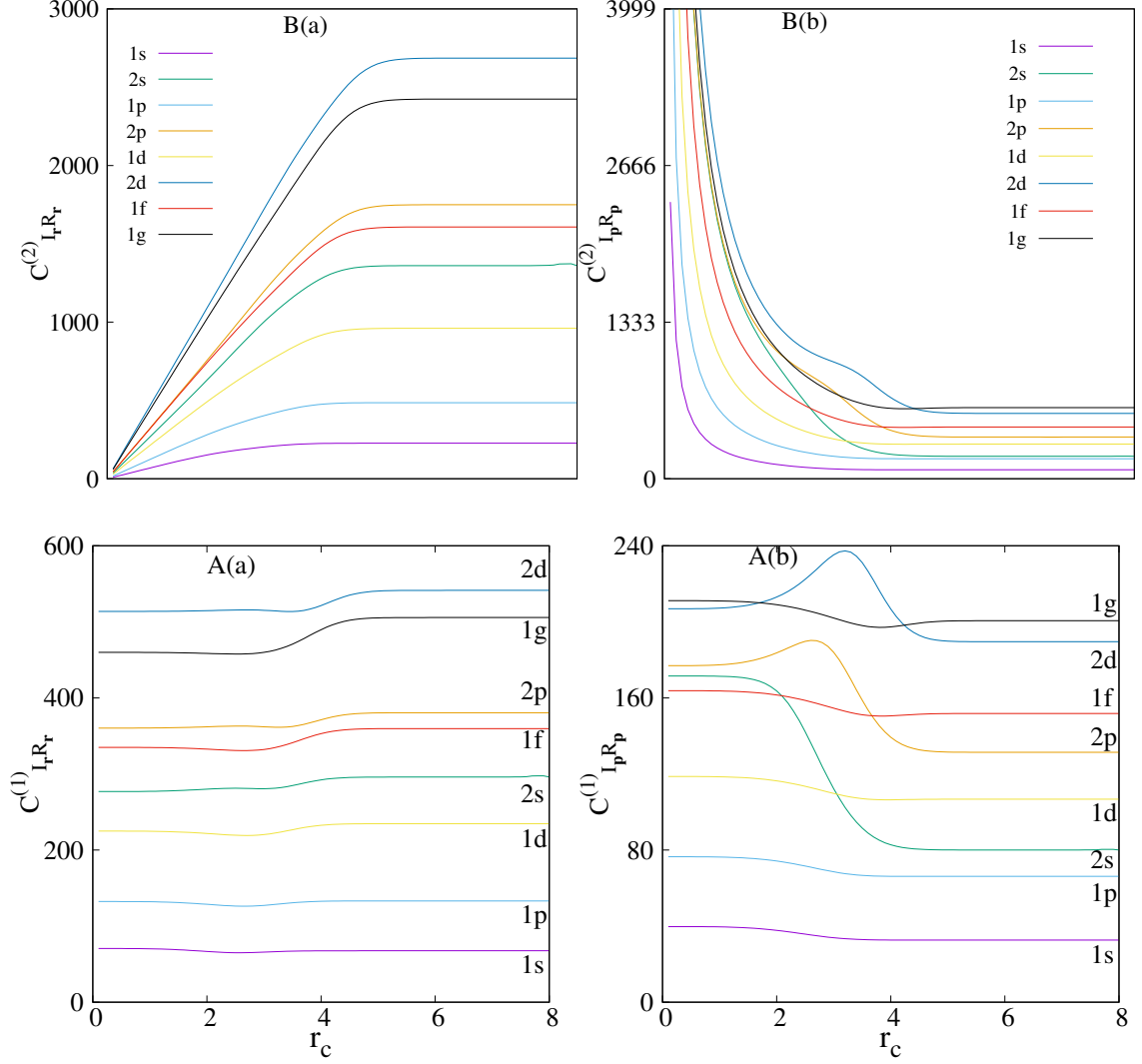


FIG. 4: Plots of  $C_{I_r R_r}^{(1)}$ ,  $C_{I_p R_p}^{(1)}$  (bottom row A) and  $C_{I_r R_r}^{(2)}$ ,  $C_{I_p R_p}^{(2)}$  (top row B) in CHO with  $r_c$  for  $1s, 1p, 1d, 2s, 1f, 2p, 1g, 2d$  states. For further details, see text.

$C_{E_p S_p}^{(1)}$  with respect to dependence of quantum numbers  $n$ ,  $l$ . Hence, in practice  $C_{ER}^{(1)}$  may possibly be considered a better measure of complexity than  $C_{ES}^{(1)}$ .

In Fig. 3, lower  $\{A(a), A(b)\}$  and upper  $\{B(a), B(b)\}$  panels depict the alteration of  $\{C_{I_r S_r}^{(1)}, C_{I_p S_p}^{(1)}\}$  and  $\{C_{I_r S_r}^{(2)}, C_{I_p S_p}^{(2)}\}$  with rise in  $r_c$  for all the states mentioned above. Nature of variation of  $\{C_{I_r S_r}^{(1)}, C_{I_p S_p}^{(1)}\}$  with  $r_c$  changes from state to state. From lower panels it is gathered that, at a fixed  $n$ , both  $C_{I_r S_r}^{(1)}$  and  $C_{I_p S_p}^{(1)}$  elevate with  $l$ . Similarly from panel A(c) in Fig. S3 of SM one can infer that, at a certain  $n$ ,  $C_{I_t S_t}^{(1)}$  increases with growth of  $l$ . On the other hand, the top panels B(a) and B(b) portray that, for these states  $C_{I_r S_r}^{(2)}$  and  $C_{I_p S_p}^{(2)}$  progress and regress with growth in  $r_c$  and finally approach to respective IHO values. Like

TABLE IV:  $C_{I_r R_r}^{(2)}$ ,  $C_{I_p R_p}^{(2)}$  and  $C_{I_t R_t}^{(2)}$  for  $1s$ ,  $2s$ ,  $1p$ ,  $1d$  states in CHO at various  $r_c$ .

$r_c$	$C_{I_r R_r}^{(2)}$	$C_{I_p R_p}^{(2)}$	$C_{I_t R_t}^{(2)}$	$C_{I_r R_r}^{(2)}$	$C_{I_p R_p}^{(2)}$	$C_{I_t R_t}^{(2)}$
	$1s$			$2s$		
0.1	9.433173	2356.25770	22226.98694	36.667294	19837.6528	727393.0643
0.2	18.866136	1178.12662	22226.69794	73.334753	9918.7949	727392.3819
0.5	47.144086	471.21450	22214.97745	183.353522	3967.0032	727364.0186
0.8	75.237916	294.38160	22148.65828	293.516420	2477.4726	727178.9180
1.0	93.643707	235.33582	22037.71925	367.211469	1979.1660	726772.4766
2.5	196.075111	93.44035	18321.32860	939.702768	589.5390	553991.4457
5.0	226.884302	76.15910	17279.30538	1360.441254	191.4695	260483.1381
7.0	226.88661187	76.1582577	17279.28906	1360.840385	191.307601	260358.110977
	$1p$			$1d$		
0.1	16.937866	5462.96222	92530.92231	29.265843	9760.87960	285660.37271
0.2	33.875565	2731.47795	92530.35998	58.531547	4880.43593	285659.46552
0.5	84.672004	1092.53992	92507.54481	146.314712	1952.11162	285622.65198
0.8	135.321527	682.65619	92378.07852	233.974746	1219.84752	285413.51636
1.0	168.827692	545.88248	92160.08039	292.195994	975.57961	285060.45712
2.5	384.346677	216.47518	83201.51983	695.405048	386.96541	269097.70008
5.0	485.702587	170.28809	82709.36712	960.529605	294.68695	283055.54874
7.0	485.72457911	170.2950413	82716.48726	960.6865379473	294.7369698	283149.8391222

the previous cases, panel B(c) in Fig. S3 shows the plot of  $C_{I_t S_t}^{(2)}$  versus  $r_c$ . From panels {B(a), B(b)} one observes that, at a particular  $n$  both  $C_{I_r S_r}^{(2)}$ ,  $C_{I_p S_p}^{(2)}$  increase with advancement in  $l$ . Also, at a certain  $l$ , they enhance with improvement of  $n$ . A careful study of Figs. 3 and S3 express that, in case of CHO,  $\{C_{I_r S_r}^{(2)}, C_{I_p S_p}^{(2)}, C_{I_t S_t}^{(2)}\}$  offer more transparent pattern than  $\{C_{I_r S_r}^{(1)}, C_{I_p S_p}^{(1)}, C_{I_t S_t}^{(1)}\}$ . So, in order to get a quantitative idea,  $\{C_{I_r S_r}^{(2)}, C_{I_p S_p}^{(2)}, C_{I_t S_t}^{(2)}\}$  values at eight different  $r_c$ 's are provided in Tables III ( $1s$ ,  $1p$ ,  $2s$ ,  $1d$ ) and S3 ( $2p$ ,  $2d$ ,  $1f$ ,  $1g$ ). Again no results are available in literature.

Finally, in Fig. 4 the bottom (A(a),A(b)) and top (B(a)-B(b)) panels provide the behavioral pattern in our last complexity measure, *viz.*,  $C_{I_r R_r}^{(1)}$ ,  $C_{I_p R_p}^{(1)}$  and  $C_{I_r R_r}^{(2)}$ ,  $C_{I_p R_p}^{(2)}$  with variations in  $r_c$ . Panel A(a) reveals that,  $C_{I_r R_r}^{(1)}$  progresses slowly with  $r_c$  to attain the IHO values. At a suitable  $n$  this quantity advances with  $l$ . In a parallel manner, at a constant  $l$ ,  $C_{I_r R_r}^{(1)}$  accumulates with  $n$ . Besides this, panel A(b) shows that, for circular states ( $1s$ ,  $1p$ ,  $1d$ ,  $1f$ ,  $1g$ )  $C_{I_p R_p}^{(1)}$  diminishes with progression in  $r_c$ . But for states having one radial node ( $2s$ ,  $2p$ ,  $2d$ ) there appears a maximum in  $C_{I_p R_p}^{(1)}$ . This maximum gets right shifted with increase in  $l$ . Now, panel A(c) of Fig. S4 implies that, the dependence of  $C_{I_t R_t}^{(1)}$  on  $r_c$  changes state-wise. Panels B(a), B(b) promptly portray that,  $C_{I_r R_r}^{(2)}$ ,  $C_{I_p R_p}^{(2)}$ , accelerate and

decelerate respectively with growth of  $r_c$ . Further, at a fixed  $n$ , both  $C_{I_r R_r}^{(2)}$ ,  $C_{I_p R_p}^{(2)}$  enhance with emergence of  $l$ . Finally, panel B(c) of Fig. S4 in SM displays the trend of  $C_{I_t R_t}^{(2)}$  with improvement of  $r_c$ . A closer investigation of Figs. 4 and S4 conveys that,  $C_{I_r R_r}^{(2)}$ ,  $C_{I_p R_p}^{(2)}$ ,  $C_{I_t R_t}^{(2)}$  characterizes CHO better than  $C_{I_r R_r}^{(1)}$ ,  $C_{I_p R_p}^{(1)}$ ,  $C_{I_t R_t}^{(1)}$ . Thus, former three measures are given in Tables IV and S4, at some appropriately chosen  $r_c$  for which no direct comparison could be made. It is hoped that, this study would be useful in future and inspires further work.

#### IV. FUTURE AND OUTLOOK

Four different complexity measures namely  $C_{ES}$ ,  $C_{IS}$ ,  $C_{ER}$ ,  $C_{IR}$  are investigated for some low-lying states of CHO in composite  $r$  and  $p$  spaces, keeping  $m$  fixed at zero. We have performed the calculations using a global quantity ( $E$ ) and a local quantity ( $I$ ). Both these may be used as measure of *order* in a system. All these results are reported here for the first time. Sensitivity of such measures depends on the nature of the particular quantum system under investigation. It is found that,  $C_{ES}^{(1)}$ ,  $C_{ER}^{(1)}$  offer more explicit explanation than  $C_{ES}^{(2)}$ ,  $C_{ER}^{(2)}$  about a given system. On the other side,  $C_{IS}^{(2)}$ ,  $C_{IR}^{(2)}$  infer the behavior of CHO more efficiently compared to  $C_{IS}^{(1)}$ ,  $C_{IR}^{(1)}$ . Hence, considering the nature of complexity measures, it is worthwhile to determine the appropriate value of  $b$ . Accurate results for  $C_{ES}^{(1)}$ ,  $C_{ER}^{(1)}$ ,  $C_{IS}^{(2)}$ ,  $C_{IR}^{(2)}$  are provided for first eight states of CHO. Further, an investigation of all these quantities in the realm of Rydberg states under different kinds of soft confined environment may be worthwhile pursuing.

#### V. ACKNOWLEDGEMENT

Financial support from DST SERB, New Delhi, India (sanction order: EMR/2014/000838) is gratefully acknowledged. NM thanks DST SERB, New Delhi, India, for a National-post-doctoral fellowship (sanction order: PDF/2016/000014/CS).

---

[1] A. Michels, J. de Boer and A. Bijl, *Physica* **4**, 981 (1937).

- [2] J. R. Sabin, E. Brändas and S. A. Cruz (Eds.), *The Theory of Confined Quantum Systems*, Parts I and II, Advances in Quantum Chemistry, Vols. 57 and 58 (Academic Press, Cambridge, Massachusetts, 2009).
- [3] K. D. Sen (Ed.), *Electronic Structure of Quantum Confined Atoms and Molecules*, (Springer, Switzerland, 2014).
- [4] O. A. Rosso, M. T. Martin and A. Plastino, *Physica A* **320**, 497 (2003).
- [5] C. R. Shalizi, K. L. Shalizi and R. Haslinger, *Phys. Rev. Lett.* **93**, 118701 (2004).
- [6] K. Ch. Chatzisavvas, Ch. C. Moustakidis and C. P. Panos, *J. Chem. Phys.* **123**, 174111 (2005).
- [7] P. A. Bouvrie, J. C. Angulo and J. S. Dehesa, *Physica A* **390**, 2215 (2011).
- [8] N. Goldenfeld and L. P. Kadanoff, *Science* **284**, 87 (1999).
- [9] K. D. Sen (Ed.), *Statistical Complexity: Applications in Electronic Structure*, (Springer, Berlin, Germany, 2012).
- [10] P. T. Landsberg, *Phys. Lett. A* **102**, 171 (1984).
- [11] P. T. Landsberg and J. S. Shiner, *Phys. Lett. A* **245**, 228 (1998).
- [12] J. S. Shiner, M. Davison and P. T. Landsberg, *Phys. Rev. E* **59**, 1459 (1999).
- [13] R. López-Ruiz, H. L. Mancini and X. Calbet, *Phys. Lett. A* **209**, 321 (1995).
- [14] C. Anteneodo and A. R. Plastino, *Phys. Lett. A* **223**, 348 (1996).
- [15] R. G. Catalán, J. Garay and R. López-Ruiz, *Phys. Rev. E* **66**, 011102 (2002).
- [16] J. R. Sánchez and R. López-Ruiz, *Physica A* **355**, 633 (2005).
- [17] E. Romera and J. S. Dehesa, *J. Chem. Phys.* **120**, 8906 (2004).
- [18] K. D. Sen, J. Antolín and J. C. Angulo, *Phys. Rev. A* **76**, 032502 (2007).
- [19] J. C. Angulo, J. Antolín and K. D. Sen, *Phys. Lett. A* **372**, 670 (2008).
- [20] J. S. Dehesa, P. Sánchez-Moreno and R. J. Yáñez, *J. Comput. Appl. Math.* **186**, 523 (2006).
- [21] J. Antolín and J. C. Angulo, *Int. J. Quant. Chem.* **109**, 586 (2009).
- [22] X. Calbet, R. López-Ruiz, *Phys. Rev. E* **63**, 066116 (2001).
- [23] M. T. Martin, A. Plastino and A. O. Rosso, *Physica A* **369**, 439 (2006).
- [24] E. Romera and Á. Nagy, *Phys. Lett. A* **372**, 6823 (2008).
- [25] R. López-Ruiz, Á. Nagy, E. Romera and J. Sañudo, *J. Math. Phys.* **50**, 123528 (2009).
- [26] E. Romera, K. D. Sen and Á. Nagy, *J. Stat. Mech.* **2011**, P09016 (2011).
- [27] D. P. Feldman and J. P. Crutchfield, *Phys. Lett. A* **238**, 244 (1998).
- [28] R. López-Ruiz, *Biophys. Chem.* **115**, 215 (2005).

- [29] T. Yamano, J. Math. Phys. **45**, 1974 (2004).
- [30] T. Yamano, Physica A **340**, 131 (2004).
- [31] Á. Nagy and E. Romera, Physica A **391**, 3650 (2012).
- [32] E. Romera, M. Calixto and Á. Nagy, J. Mol. Model. **20**, 2237 (2014).
- [33] J. C. Angulo and J. Antolín, J. Chem. Phys. **128**, 164109 (2008).
- [34] J. B. Szabó, K. D. Sen and Á. Nagy, Phys. Lett. A **372**, 2428 (2008).
- [35] J. Sañudo and R. López-Ruiz, J. Phys. A **41**, 265303 (2008).
- [36] Á. Nagy, K. D. Sen and H. E. Montgomery Jr., Phys. Lett. A **373**, 2552 (2009).
- [37] E. Romera, R. López-Ruiz, J. Sañudo and Á. Nagy, Int. Rev. Phys. **3**, 207 (2009).
- [38] S. Majumdar, N. Mukherjee and A. K. Roy, Chem. Phys. Lett. **687**, 322, (2017).
- [39] H. E. Montgomery Jr., N. A. Aquino and K. D. Sen, Int. J. Quant. Chem. **107**, 798 (2007).
- [40] A. K. Roy, J. Phys. G **30**, 269 (2004).
- [41] K. D. Sen and A. K. Roy, Phys. Lett. A **357**, 112 (2006).
- [42] A. K. Roy, Int. J. Quant. Chem. **115**, 937 (2015); *ibid.*, **116**, 953 (2016).
- [43] N. Mukherjee and A. K. Roy, Int. J. Quant. Chem. e25596 (2018).
- [44] E. Romera, P. Sánchez-Moreno and J. S. Dehesa, Chem. Phys. Lett. **414**, 468, (2005).
- [45] A. K. Roy, A. F. Jalbout and E. I. Proynov, Int. J. Quant. Chem. **108**, 827 (2008).



## Supplemental Materials: Various Complexity measures in confined isotropic harmonic oscillator.

TABLE S1:  $C_{E_r S_r}^{(1)}$ ,  $C_{E_p S_p}^{(1)}$  and  $C_{E_t S_t}^{(2)}$  for  $2p$ ,  $1f$ ,  $2d$ ,  $1g$  states in CHA at various  $r_c$ .

$r_c$	$C_{E_r S_r}^{(1)}$	$C_{E_p S_p}^{(1)}$	$C_{E_t S_t}^{(1)}$	$C_{E_r S_r}^{(1)}$	$C_{E_p S_p}^{(1)}$	$C_{E_t S_t}^{(1)}$
	$2p$			$1f$		
0.1	17.254949	0.01082	0.01082	13.123129	0.01427	0.18738
0.2	8.6274798	0.02167	0.02167	6.5615707	0.02855	0.18738
0.5	3.4510731	0.05417	0.05417	2.6247241	0.07139	0.18738
0.8	2.1572081	0.08663	0.08663	1.6407953	0.11417	0.18733
1.0	1.7261513	0.10817	0.10817	1.3131066	0.14261	0.18726
2.5	0.6957840	0.25900	0.25900	0.5416028	0.34020	0.18425
5.0	0.5147727	0.51412	0.51412	0.4457094	0.44582	0.19870
7.0	0.5147878061	0.5147737557	0.2649992523	0.445715446	0.445715446	0.1986622588
	$2d$			$1g$		
0.1	16.873312	0.01093	0.18443	13.851781	0.01323	0.18332
0.2	8.4366593	0.02186	0.18443	6.9258936	0.02646	0.18332
0.5	3.3747169	0.05466	0.18449	2.7704060	0.06617	0.18333
0.8	2.1093871	0.08742	0.18441	1.7316772	0.10584	0.18328
1.0	1.6877640	0.10920	0.18430	1.3855802	0.13222	0.18321
2.5	0.6790658	0.25869	0.17567	0.5629633	0.31866	0.17939
5.0	0.4658442	0.46532	0.21676	0.4323887	0.43266	0.18708
7.0	0.4658988655	0.4658839758	0.2170548158	0.4324104301	0.4324104287	0.1869787794

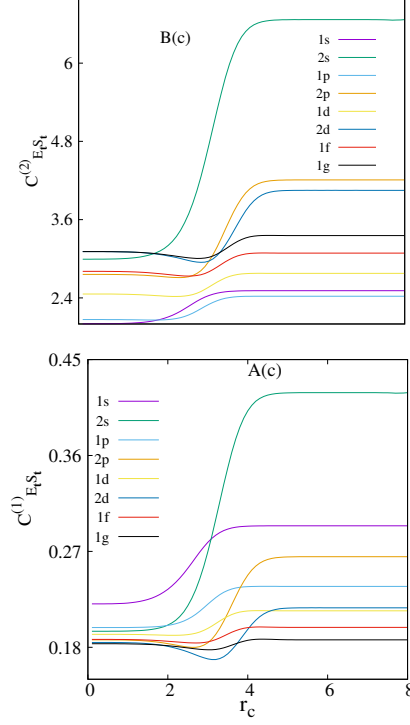


FIG. S1: Variation of  $C_{E_t S_t}^{(1)}$  (bottom panel) and  $C_{E_t S_t}^{(2)}$  (top panel) in CHA with  $r_c$ , for  $1s, 1p, 1d, 2s, 1f, 2p, 1g, 2d$  states. See text for details.

TABLE S2:  $C_{E_r R_r}^{(1)}$ ,  $C_{E_p R_p}^{(1)}$  and  $C_{E_t R_t}^{(1)}$  for  $2p, 1f, 2d, 1g$  states in CHA at various  $r_c$ .

$r_c$	$C_{E_r R_r}^{(1)}$	$C_{E_p R_p}^{(1)}$	$C_{E_t R_t}^{(1)}$	$C_{E_r R_r}^{(1)}$	$C_{E_p R_p}^{(1)}$	$C_{E_t R_t}^{(1)}$
	<i>2p</i>			<i>1f</i>		
0.1	21.962364	0.00750	0.16484	15.469104	0.00778	0.12044
0.2	10.981186	0.01501	0.16484	7.7345610	0.01557	0.12044
0.5	4.3925400	0.03754	0.16490	3.0939653	0.03893	0.12045
0.8	2.7455678	0.06006	0.16489	1.9342326	0.06228	0.12047
1.0	2.1967578	0.07505	0.16488	1.5480782	0.07784	0.12050
2.5	0.8799189	0.18327	0.16126	0.6434298	0.19071	0.12271
5.0	0.6848110	0.23658	0.16201	0.5730916	0.24199	0.13868
7.0	0.6852179489	0.236635087	0.1621466089	0.5732802278	0.2419896511	0.1387278823
	<i>2d</i>			<i>1g</i>		
0.1	21.252468	0.00653	0.13879	16.403268	0.00670	0.11001
0.2	10.626237	0.01306	0.13880	8.2016383	0.01341	0.11001
0.5	4.2505534	0.03265	0.13880	3.2807273	0.03353	0.11001
0.8	2.6568022	0.05224	0.13881	2.0507122	0.05364	0.11001
1.0	2.1257180	0.06531	0.13883	1.6409239	0.06705	0.11002
2.5	0.8533617	0.16032	0.13681	0.6693462	0.16545	0.11074
5.0	0.6135813	0.21513	0.13200	0.5534133	0.21974	0.12160
7.0	0.6145939107	0.2152218204	0.1322740202	0.5538899983	0.2197225423	0.1217021186

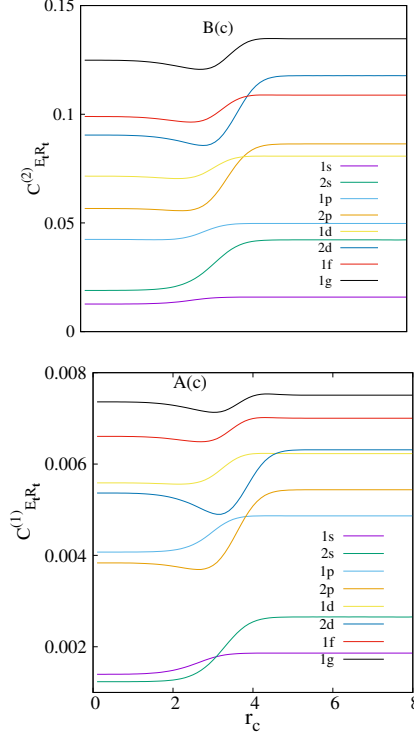


FIG. S2: Variation of  $C_{E_t R_t}^{(1)}$  (bottom panel) and  $C_{E_t R_t}^{(2)}$  (top panel) in CHA with  $r_c$ , for  $1s, 1p, 1d, 2s, 1f, 2p, 1g, 2d$  states. See text for details.

TABLE S3:  $C_{I_r S_r}^{(2)}$ ,  $C_{I_p S_p}^{(2)}$  and  $C_{I_t S_t}^{(2)}$  for  $2p, 1f, 2d, 1g$  states in CHA at various  $r_c$ .

$r_c$	$C_{I_r S_r}^{(2)}$	$C_{I_p S_p}^{(2)}$	$C_{I_t S_t}^{(2)}$	$C_{I_r S_r}^{(2)}$	$C_{I_p S_p}^{(2)}$	$C_{I_t S_t}^{(2)}$
	$2p$			$1f$		
0.1	30.829956	34610.5200	1067040.8207	34.277127	37301.84939	1278600.25861
0.2	61.659980	17305.3029	1067044.6459	68.554152	18650.87667	1278595.04195
0.5	154.156885	6922.8172	1067199.9473	171.374909	7459.57109	1278383.32131
0.8	246.714192	4329.2398	1068084.9095	274.104430	4659.46290	1277179.42905
1.0	308.526800	3466.7631	1069589.3417	342.427973	3723.82715	1275142.58518
2.5	787.931963	1469.5392	1157896.9377	825.488912	1420.15678	1172323.68189
5.0	1139.307518	1139.8799	1298673.8182	1102.110821	1101.94896	1214469.87865
7.0	1139.373375	1139.3700	1298167.8422	1102.13885453152	1102.138856	1214710.056286
	$2d$			$1g$		
0.1	45.282593	52555.6478	2379856.0599	46.765278	58691.73842	2744735.48228
0.2	90.565221	26277.8642	2379860.5853	93.530491	29345.80827	2744727.86739
0.5	226.416428	10511.8007	2380044.3842	233.819602	11737.33406	2744418.78878
0.8	362.297120	6572.2143	2381094.3330	374.050977	7332.31702	2742660.35412
1.0	452.937222	5260.9704	2382889.3444	467.435489	5861.09040	2739681.66713
2.5	1142.740818	2202.1192	2516451.5223	1148.845130	2247.53126	2582065.35261
5.0	1772.010616	1774.2077	3143915.0074	1671.968506	1671.30118	2794362.95082
7.0	1772.5172372	1772.54450	3141865.67995	1672.1632856887	1672.16328864	2796130.05894028

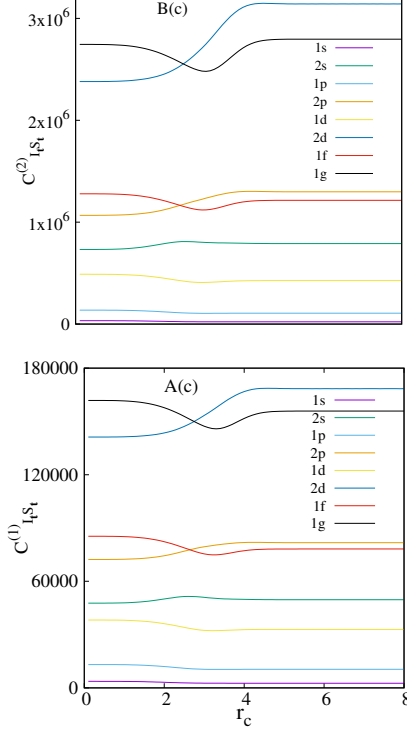


FIG. S3: Variation of  $C_{I_t S_t}^{(1)}$  (bottom panel) and  $C_{I_t S_t}^{(2)}$  (top panel) in CHA with  $r_c$ , for  $1s, 1p, 1d, 2s, 1f, 2p, 1g, 2d$  states. See text for details.

TABLE S4:  $C_{I_r R_r}^{(2)}$ ,  $C_{I_p R_p}^{(2)}$  and  $C_{I_t R_t}^{(2)}$  for  $2p, 1f, 2d, 1g$  states in CHA at various  $r_c$ .

$r_c$	$C_{I_r R_r}^{(2)}$	$C_{I_p R_p}^{(2)}$	$C_{I_t R_t}^{(2)}$	$C_{I_r R_r}^{(2)}$	$C_{I_p R_p}^{(2)}$	$C_{I_t R_t}^{(2)}$
			$2p$			
0.1	44.271169	19970.5174	884118.1701	43.867820	15021.73056	658970.57651
0.2	88.542409	9985.3085	884123.2806	87.735537	7510.86091	658969.42157
0.5	221.363121	3994.9328	884330.7969	219.328424	3004.27340	658922.55152
0.8	354.245464	2499.7145	885512.5259	350.830623	1877.41927	658656.17667
1.0	442.942959	2003.6869	887519.0282	438.337433	1501.59674	658206.06330
2.5	1120.574981	874.6934	980159.6435	1068.910611	596.06551	637140.75398
5.0	1748.130191	355.5763	621593.7685	1606.880150	440.68957	708135.33589
7.0	1749.712868	355.093236	621311.205169	1607.68230133	440.9049523	708835.0883814
			$2d$			
0.1	64.009563	24273.2716	1553721.5208	60.264374	21170.66473	1275836.85768
0.2	128.019163	12136.6807	1553727.7205	120.528683	10585.32761	1275835.60452
0.5	320.051676	4855.4017	1553979.4627	301.315183	4234.05396	1275784.74865
0.8	512.117124	3037.2289	1555416.9651	482.044895	2646.01023	1275495.72562
1.0	640.219512	2433.3390	1557871.1491	602.430376	2116.43936	1275007.36035
2.5	1609.829117	1074.3700	1729552.1569	1489.421348	840.86097	1252396.28603
5.0	2678.634631	557.7446	1493994.0015	2420.979640	604.92919	1464521.26703
7.0	2685.563139	556.522132	1494575.284942	2424.207149829	605.68437	1468304.38029

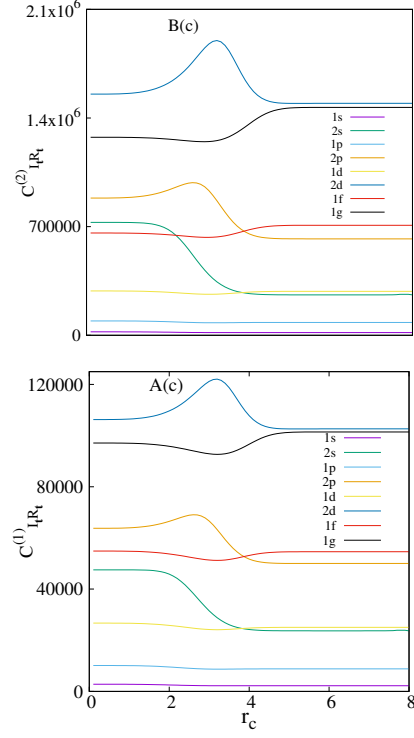


FIG. S4: Variation of  $C_{I_t R_t}^{(1)}$  (bottom panel) and  $C_{I_t R_t}^{(2)}$  (top panel) in CHA with  $r_c$ , for  $1s, 1p, 1d, 2s, 1f, 2p, 1g, 2d$  states. See text for details.